PTC&B

Potential Screening of Bioherbicidal Activity of Sapodilla (*Manilkara zapota* L.) through Molecular Docking and Dynamic Simulation

Tonema Mahmud Ema, Sohanur Rahman, Nasrin Akter, Rahi Jannat Rida, Shaikh Mizanur Rahman and Md. Abdur Rauf Sarkar*

Department of Genetic Engineering and Biotechnology, Faculty of Biological Science and Technology, Jashore University of Science and Technology, Jashore-7408, Bangladesh

Abstract

The excessive use of synthetic herbicides has raised environmental and health concerns, necessitating the search for eco-friendly alternatives. Sapodilla (*Manilkara zapota* L.), has shown potential as a natural herbicide due to its reported phytotoxic effects. This study evaluates the bioherbicidal potential of *M. zapota* leaf crude extract and investigates the molecular mechanism of its bioactive compounds through Molecular Docking (MD) and Molecular Dynamic Simulations (MDS). MD were performed to analyze the binding affinity of key phytochemicals with essential plant growth-related enzymes, such as acetohydroxyacid synthase (AHAS), cellulose synthase (CS), glutamine synthase (GLS) and the D1 protein of photosystem II (PSIID1). The analyses confirmed the strong interaction of specific bioactive compounds with target enzymes, suggesting their potential as natural herbicidal agents. The herbicidal effects of *M. zapota* extracts were assessed on selected weed species *Parthenium hysterophorus* through seed germination inhibition. The study highlights *M. zapota* as a promising source of bioherbicidal compounds, offering an environmentally sustainable alternative to synthetic herbicides.

Introduction

Weeds are unwanted or unpleasant plants that thrive in places where they are not purposefully planted. They usually compete with decorative plants, grasslands, or cultivated crops. Fields, gardens, lawns, roadsides, and other disturbed places can all support the growth of weeds. They are challenging to manage since they frequently grow quickly, adapt, and are robust (Araniti et al. 2015). They result in enormous financial losses, which in large crops can reach 34%. Chemical pesticides are the most used type of weed control. It has been established, although, that excessive use of them may have

---

*Author for corresponding: <mar.sarkar@just.edu.bd>

detrimental effects on human health, animals, and the environment as well as enhance weed resistance to herbicides (Kaab et al. 2020). For instance, in 2015, 210 weed species developed pesticide resistance (Feng et al. 2019). Since phenolic crude extracts typically have multisite action, which is not the case with synthetic herbicides, they may be able to overcome weed resistances in this situation (Soltys et al. 2013). Because of these factors, researchers are trying to find a biological way to reduce the negative effects of synthetic herbicides on agricultural production (Chengxu et al. 2011).

When plant organs interact with their surroundings, they release allelopathic substances that exhibit a variety of biological activities, some of which may be included into weed control (Carvalho et al. 2019). Plants' secondary metabolism has been shown to be a practically limitless supply of substances with countless biological functions. Allelopathic substances have been studied as allelochemicals with allelopathic effects on plants, and they are typically produced via secondary routes. These factors have led to a great deal of interest in plant extracts as sources of allelochemicals used in weed control (Cordeau et al. 2016). Numerous plants demonstrated that plant extracts prevented seedling growth and weed germination (Ribeiro et al. 2015, Lim et al. 2017). However, only a few studies have demonstrated that these chemicals have herbicidal impact when applied directly to weeds after emergence.

A well-known member of the Sapotaceae family, *Manilkara zapota*, also known as Sapodilla is utilized for traditional medicinal reasons worldwide (Gam et al. 2024). Polyphenols and flavonoids, two types of antioxidant chemicals, were found in moderately high concentrations in the methanol leaf extract of *M. zapota*. The extract's strong free radical scavenging activity (IC50 of the DPPH assay) and high total antioxidant capacity showed that it had strong antioxidant qualities. With inhibitory halos ranging from 8.00 to 11.33 mm, the extract also shown a useful antibacterial action against *Bacillus cereus*, *Staphylococcus aureus*, and *Shigella boydii*. (Shahraki et al. 2023). Additionally, the extract demonstrated a strong anti-inflammatory activity (Nguyen et al. 2025). *M. zapota* contains quercetin, kaempferol and myricitrin (Shui et al. 2004) (Tulloch et al. 2020) (Fayek et al. 2012), which can suppress the seed germination and seedling growth of certain weed species (McCurdy et al. 2013) (Kaab et al. 2020).

New natural herbicides may be developed as a result of identifying the phenolic chemicals of plant extracts and researching their harmful effects on plants (Flamini 2012). In this regard, the current work uses cutting-edge analytical and computational techniques to methodically investigate *M. zapota* leaves herbicidal capability. GC-MS profiling will first be used to identify bioactive phytochemicals, giving the plant extract a thorough chemical fingerprint. Molecular docking will be used to assess the produced chemical interactions with important weed-associated target proteins in order to anticipate potential molecular inhibitory mechanisms. Molecular dynamic simulations will be used to evaluate the stability, conformational behavior, and binding efficiency of the most promising docked complexes under physiologically relevant settings in order to further validate these interactions. In order to assess the chosen compounds'

appropriateness as natural, environmentally friendly weed-management agents, their total herbicidal potential will be assessed. *Parthenium hysterophorus* was used as the test weed due to its highly invasive nature and rapid growth. It causes significant yield losses in crops and poses serious environmental and health risks.

Materials and Methods

From Baro Balia Danga village of Jashore district of Bangladesh, leaves of the *Manilkara zapota* species were collected. After that, these were thoroughly cleaned with clean water to remove surface impurities. The leaves underwent a gentle wash for surface sanitation before being left to dry. The *M. zapota* leaves were dried, ground into a fine powder, and then weighed using an electronic balance. The powdered leaves were stored in a container. The storage environment was maintained clean, cool, dark, and dry to preserve its quality. The leaves of *M. zapota* plants were dried at 60°C for 50 sec. Following an optimized method, the plant material underwent extraction and fractionation. To obtain extract, 10 grams of dried plant powder were mixed with 100 ml of methanol and shaken at 250 rpm for 72 hrs at 25°C. The methanol was then evaporated using a rotavapor under vacuum at 45°C and 140 rpm. The resulting extracts were refrigerated at 4°C until they were analyzed. The extraction process yielded between 5.29 and 29.71% of extract (Heatley 1944). Gas Chromatography-Mass Spectrometry (GC-MS) was used to analyze the chemical makeup of *M. zapota* (Fig. 1). The relative amounts of each component were determined by the size of the peaks in the GC-MS output. These results were compared to a database of known chemical spectra (NIST-National Institute of Standards and Technology library) to identify the specific compounds present.
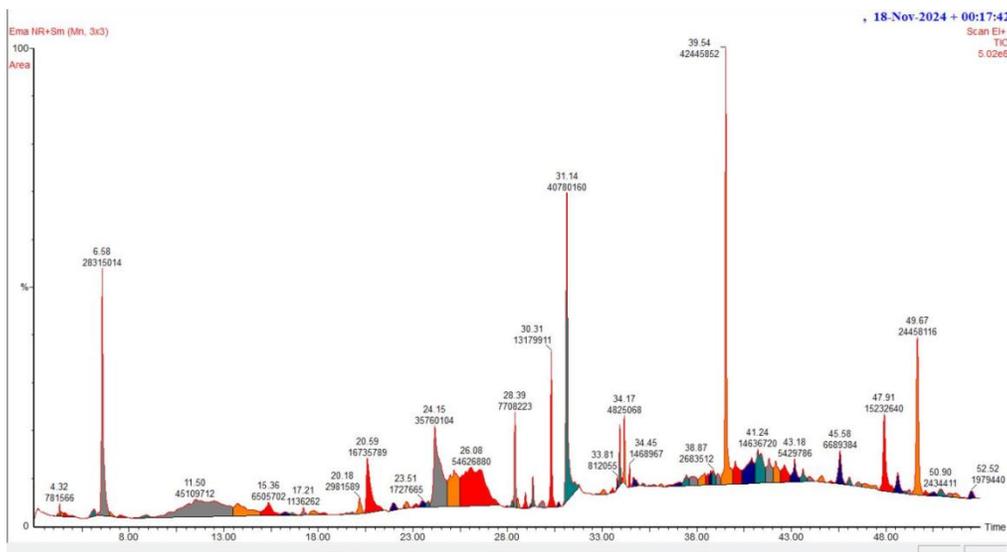

Fig. 1. GC-MS chromatogram obtained from the methanol extract of *Manilkara zapota* leaves.

Protein sequences for target receptors in weeds were obtained from the NCBI database (https://www.ncbi.nlm.nih.gov/). The 3D structures of key target proteins, including, Acetohydroxyacid Synthase (AHAS), Cellulose Synthase, Glutamine Synthase, and the D1 protein of Photosystem II, were generated using AlphaFold3-the latest version of DeepMind's AI system, which offers enhanced accuracy in protein structure prediction (Mandels et al. 2003). These proteins-AHAS, Cellulose Synthase, Glutamine Synthase, and the D1 protein of Photosystem II are essential and conserved across most weed plants, including *Amaranthus sp.* (Nandula et al. 2020). Imidazolinone and sulfonylurea synthetic herbicides inhibit acetohydroxyacid synthase (AHAS) (Stidham 1991). Dichlobenil and isoxaben inhibit cellulose synthase (Sabba et al. 1999). Triazine and benzothiadiazole herbicides inhibit Photosystem II (Teixeira et al. 2024), while glufosinate inhibits glutamine synthetase (Donn et al. 2002). Based on these well-established herbicides mode of action, the corresponding target proteins were selected to evaluate inhibition by natural bioherbicides. The target proteins play critical roles in amino acid biosynthesis, cell wall formation, nitrogen metabolism, and photosynthesis, respectively, making them suitable and relevant targets for studying herbicidal activity. These herbicide-target proteins share conserved cores and motifs in both weeds and crops (Shah et al. 2022). Many studies use crop or model plant structures as templates for herbicide docking including Pea PSII D1 (*P. sativum*) for docking commercial PSII herbicides (Battaglino et al. 2021), Rice ALS for imidazolinone docking (Buffon et al. 2020). The 3D structures were predicted based on sequences obtained from NCBI (Table 1) and subsequently prepared using the Protein Preparation Wizard in Maestro 22-4 (Bailey et al. 1976). The protein structures were refined using standard settings. This involved assigning bond orders, adding any missing hydrogen atoms and side chains, and removing all water molecules. The 3D structures of bioactive compounds, including glyphosate (CID: 3496), were downloaded from PubChem (https://pubchem.ncbi.nlm.nih.gov/). These compounds were then prepared using the LigPrep tool in Maestro 22-4, which also optimized the chemical and protein structures using the OPLS_2005 force field.

Table 1. Fasta formats of the protein sequences of the selected proteins.

Sl. No.	Protein Name	Fasta Formats (Protein Sequences)
1	Acetohydroxyacid synthase	>UZC82024.1 acetohydroxyacid synthase, partial [Brassica napus]
2	Cellulose synthase	>AAL23710.2 cellulose synthase [Populus tremuloides]
3	Glutamine synthase	>BAB02705.1 glutamine synthase [Arabidopsis thaliana]
4	Photosystem II protein D1	>NP_043004.1 photosystem II protein D1 (chloroplast) [Zea mays]

Molecular docking is a valuable tool for understanding how proteins and ligands interact. In this research, the Glide module within the Schrödinger Suite was used to simulate the binding of natural compounds (identified through GC-MS) to the target proteins. The docking procedure was conducted in standard precision mode, utilizing

the OPLS_2005 force field for energy minimization and accuracy. To determine the optimal binding site, the native inhibitor compounds were analyzed in complex with their respective target receptors. Based on this analysis, a receptor grid was generated using binding site residues. The resulting grid box coordinates for each protein were as follows:

1. Acetohydroxyacid Synthase (AHAS): X = 63.66, Y = -62.36, Z = -12.58
2. Cellulose Synthase (CS): X = -44.75, Y = -32.69, Z = -18.78
3. Glutamine Synthase (GLS): X = 18.63, Y = -2.05, Z = -6.6
4. D1 protein of Photosystem II (PSIID1): X = -26.41, Y = -2.25, Z = 36.37

These docking simulations enabled the calculation of binding energies between the ligands and their respective protein targets. The entire A chain of the target proteins was used as receptor for all the compounds to bind through docking. The Maestro viewer was used to visualize the interactions between the ligands and proteins, including the specific amino acid residues involved in binding and the types of chemical bonds formed.

The stability of the protein-ligand complexes was evaluated under physiological conditions using 50-nanosecond molecular dynamics (MD) simulations with the Desmond package (Schrödinger Suite). The initial protein-ligand complex structures, derived from molecular docking, were prepared using the Protein Preparation Wizard. An orthorhombic periodic boundary box ($10 \times 10 \times 10$ Å^3) was used to define the system volume. The complexes were solvated with SPC water, and 0.15 M NaCl was added. Energy minimization and relaxation were performed using the OPLS_2005 force field. The production MD run used an NPT ensemble (1.01325 bar, 300 K). After equilibration, data were recorded every 150 picoseconds. The radius of gyration (rGyr), solvent-accessible surface area (SASA), root-mean-square deviation (RMSD), and root-mean-square fluctuation (RMSF) were calculated to assess complex dynamics and stability. The simulations were run on a system with Ubuntu 20.04.1 LTS, an Intel Core i7-10700K processor, 64GB DDR4 RAM, and an RTX 3060Ti GPU.

The seeds of *Parthenium hysterophorus* were collected and placed in two Petri dishes. One dish was designated for treatment with the extract, while the other served as the control. A total of 45 seeds were soaked in water and arranged on sterile tissue paper to facilitate germination, preparing them for the pre-emergence test. The extract of *M. zapota* leaves were used in amount of 0.5 g in solubilized with 0.04 g or 2 drops of Tween-20 and 10 ml distilled water. The germination inhibition was observed after 5 days.

Statistical analysis (e.g., t-tests) was done to determine that the germination percentages are statistically significant or not. The t-test score for seed germination percentage is 8.12. The t-distribution table was used to find the p-value. The t-test formula is $t = \dfrac{\overline{x_1} - \overline{x_2}}{\sqrt{\dfrac{s_1^2}{n_1} + \dfrac{s_2^2}{n_2}}}$

Where the,

$\overline{x_1}, \overline{x_2}$ = Sample means of groups 1(control) and 2 (Treatment)

s_1^2, s_2^2 = Sample variances of groups 1 and 2

n_1, n_2 = Sample sizes of groups 1 and 2

Results and Discussion

GC-MS analysis of *M. zapota* revealed 93 distinct peaks, each representing a unique compound (Fig. 1). Of these, 36 compounds present in the methanol extract were identified based on their retention time, peak area and compound in Table 2. These compounds were detected over a 50 min analysis period.

Table 2. List of compounds identified from methanol extract of *Manilkara zapota* leaves by GC-MS analysis.

Sl. No.	Retention time	Area%	Compound name	Compound CID
1	4.324	0.146389	CIS-2,4-DIMETHYLTHIANE, S,S-DIOXIDE	543891
2	6.575	5.303457	SUCCINIC ACID, BUTYL HEX-4-YN-3-YL ESTER	91701883
3	11.502	8.449136	3-METHYL-2-(2-OXOPROPYL)FURAN	545772
4	13.733	2.208723	CHOLEST-5-EN-3-OL, (3.ALPHA.)-, TMS DERIVATIVE	22211625
5	15.364	1.21853	CYCLOHEXASILOXANE, DODECAMETHYL-	10911
6	17.21	0.212824	TRANS-2-METHYL-4-N-PENTYLTHIANE, S,S-DIOXIDE	N/A
7	17.735	0.343219	2-[(P-TRIMETHYLSILYLOXY)PHENYL]-2-[(P-TRIMETHYLSILYLOXYETHYLENOXY)PHENYL]PROPANE	6421186
8	20.177	0.558457	TRISILOXANE, 1,1,1,5,5,5-HEXAMETHYL-3,3-BIS[(TRIMETHYLSILYL)OXY]	19086
9	20.592	3.134646	2-METHALLYL ALCOHOL, TMS DERIVATIVE	582142
10	21.932	0.418713	3',5'-DIMETHOXYACETOPHENONE	95997
11	22.663	0.235609	DODECANEDIOIC ACID, 2TMS DERIVATIVE	519943
12	24.153	6.697937	DIETHANOLNITROSAMINE, 2TMS DERIVATIVE	552927
13	25.164	3.97051	DIETHANOLNITROSAMINE, 2TMS DERIVATIVE	552927
14	26.084	10.23172	2-[(TRIMETHYLSILYL)OXY]TETRADECANOICACID,BIS(TRIMETHYLSILYL) ESTER	552442
15	28.39	1.443765	NEOPHYTADIENE	10446
16	28.946	0.370674	NEOPHYTADIENE	10446
17	29.346	0.502621	PHYTYL TETRADECANOATE	14486554
18	29.856	0.325343	2-TRIMETHYLSILOXY-6-HEXADECENOIC ACID, METHYL ESTER	91696378
19	30.311	2.468623	TETRADECANOIC ACID, 10,13-DIMETHYL-, METHYL ESTER	554145
20	31.142	7.638203	N-HEXADECANOIC ACID	985
21	33.938	0.839993	METHYL 7,11,14-EICOSATRIENOATE	91694374
22	34.173	0.903745	PHYTOL	5280435
23	34.448	0.27514	TETRADECANOIC ACID, 10,13-DIMETHYL-, METHYL ESTER	554145
24	38.87	0.502627	TETRACOSANOIC ACID	11197
25	39.536	7.95019	HEXANEDIOIC ACID, BIS(2-ETHYLHEXYL) ESTER	7641
26	40.041	1.577916	18-METHYL-NONADECANE-1,2-DIO, TRIMETHYLSILYL ETHER	91743658
27	41.236	2.741486	METHYL 2-HYDROXY-EICOSANOATE	3472786
28	41.822	1.503306	TETRACONTANE-1,40-DIOL	557624

29	43.177	1.017009	HENTRIACONTANE	12410
30	43.618	0.493909	I-PROPYL 11,12-METHYLENE-OCTADECANOATE	91692516
31	45.578	1.252935	HENTRIACONTANE	12410
32	47.915	2.853103	9-OCTADECENAMIDE	1930
33	48.63	0.878273	HENTRIACONTANE	12410
34	49.67	4.581052	SQUALENE	638072
35	50.901	0.45597	18-METHYL-NONADECANE-1,2-DIO, TRIMETHYLSILYL ETHER	91743658
36	52.522	0.370753	DOTRIACONTYL ISOPROPYL ETHER	91692940

A molecular docking study was performed to investigate the interactions and binding strength between all 36 phytochemicals and the four target proteins. All 36 phytochemicals were bound to the active site (Table 3). The 3D structures of the proteins and phytochemicals were docked using Maestro 2022-4 to determine the protein-compound binding scores (Fig. 2 and Fig. 3). The docking results were compiled in a table (Table 4), listing the docking scores below -5.00.

Table 3. Molecular docking score of the selected proteins and natural compounds of *M. zapota* was identified through GC-MS analysis and glyphosate.

Sl. No.	Acetohydroxyacid Synthase		Cellulose Synthase		Glutamine Synthase		Photosystem II D1	
	CID	Docking score	CID	Docking score	CID	Docking score	CID	Docking score
1	543891	-5.546	22211625	-7.539	95997	-7.082	95997	-7.238
2	91696378	-5.307	6421186	-6.536	6421186	-6.456	638072	-6.804
3	6421186	-4.696	95997	-5.792	3472786	-6.115	6421186	-6.647
4	545772	-4.657	543891	-5.609	91692516	-5.911	91692516	-6.542
5	3472786	-4.489	91692516	-5.045	3472786	-5.521	91696378	-6.507
6	3496 (control: Glyphosate)	-2.225	3496 (control: Glyphosate)	-3.878	3496 (control: Glyphosate)	-3.88	3496 (control: Glyphosate)	-4.074

Based on the docking scores, the top-performing compounds for each of the four target receptors were identified. Table 3 presents the molecular docking scores of the selected proteins and natural compounds of *Manilkara zapota*, as identified through GC-MS analysis, alongside glyphosate.

The PASS online tool was used to predict the potential of selected lead compounds to inhibit plant cell growth. The combined qualities of the phytochemicals were taken into account such as 1-Aminocyclopropane-1-carboxylate deaminase inhibitor, Acetolactate synthase inhibitor, Microtubule formation inhibitor, Cellulase inhibitor, Glutaminase inhibitor and ATPase inhibitor. Higher Pa values suggest stronger pharmacological activity and greater potential for experimental development. Despite its inability to forecast the binding affinity, the PASS prediction aids in minimizing the negative effects of chemicals. All the selected phytochemicals were taken for PASS prediction before the MD simulation shown in Table 5.
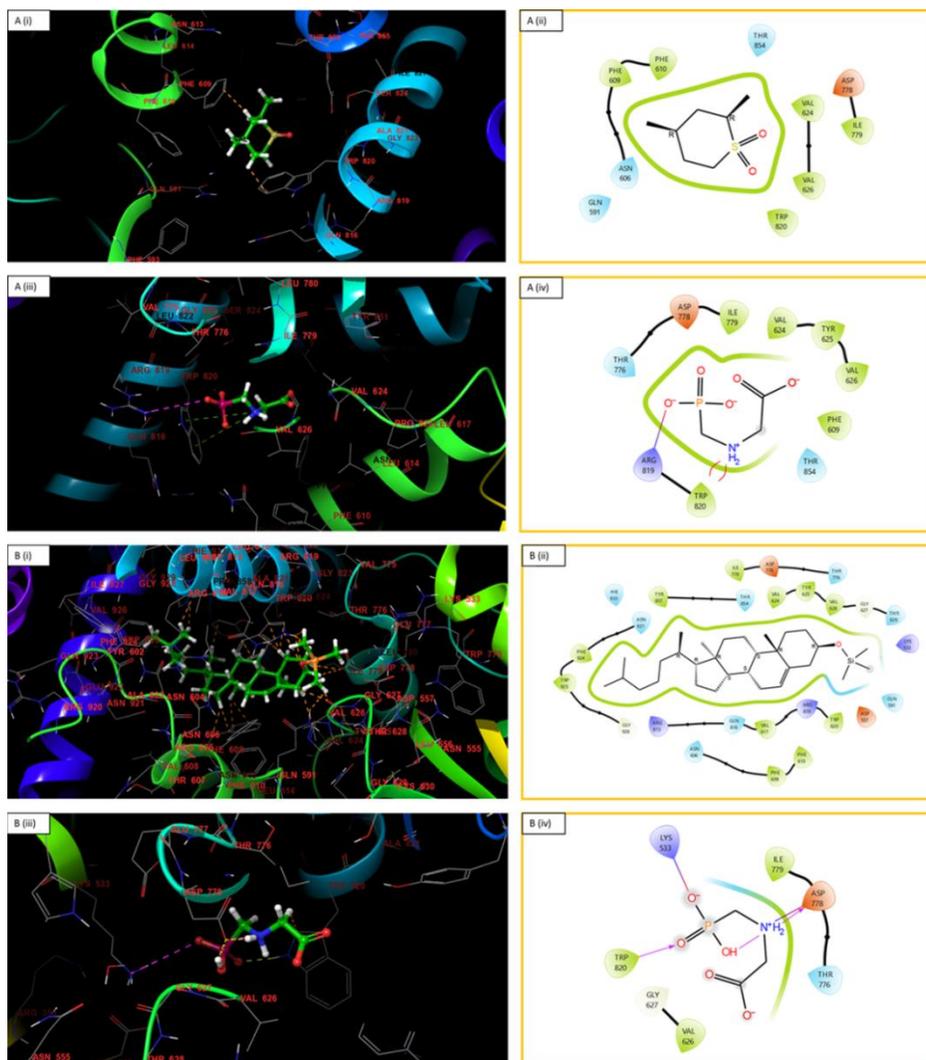
Fig. 2. Interactions between the target receptors and selected compounds representing in 3D (left) and 2D (right) format. Representing the compounds, A. AHAS (i, ii) CID: 543891, A. AHAS (iii, iv) CID: 3496 (control), B. CS (i, ii) CID: 22211625, B. CS (iii, iv) CID: 3496 (control).

Molecular dynamics (MD) simulations, a part of the computer-aided drug discovery (CADD) process, were used to quickly evaluate the stability and interactions within the protein-ligand complex (Shukla et al. 2021). In a synthetic environment, MD simulations also provide insights into the conformational shifts of complex molecular systems. Therefore, 50-nanosecond MD simulations were conducted to investigate the structural changes of proteins upon interaction with specific ligands. To analyze these interactions, final snapshots were extracted from the 50-nanosecond MD trajectories and examined for intermolecular reactions. A total of 12 MD simulations were performed, where the first 4
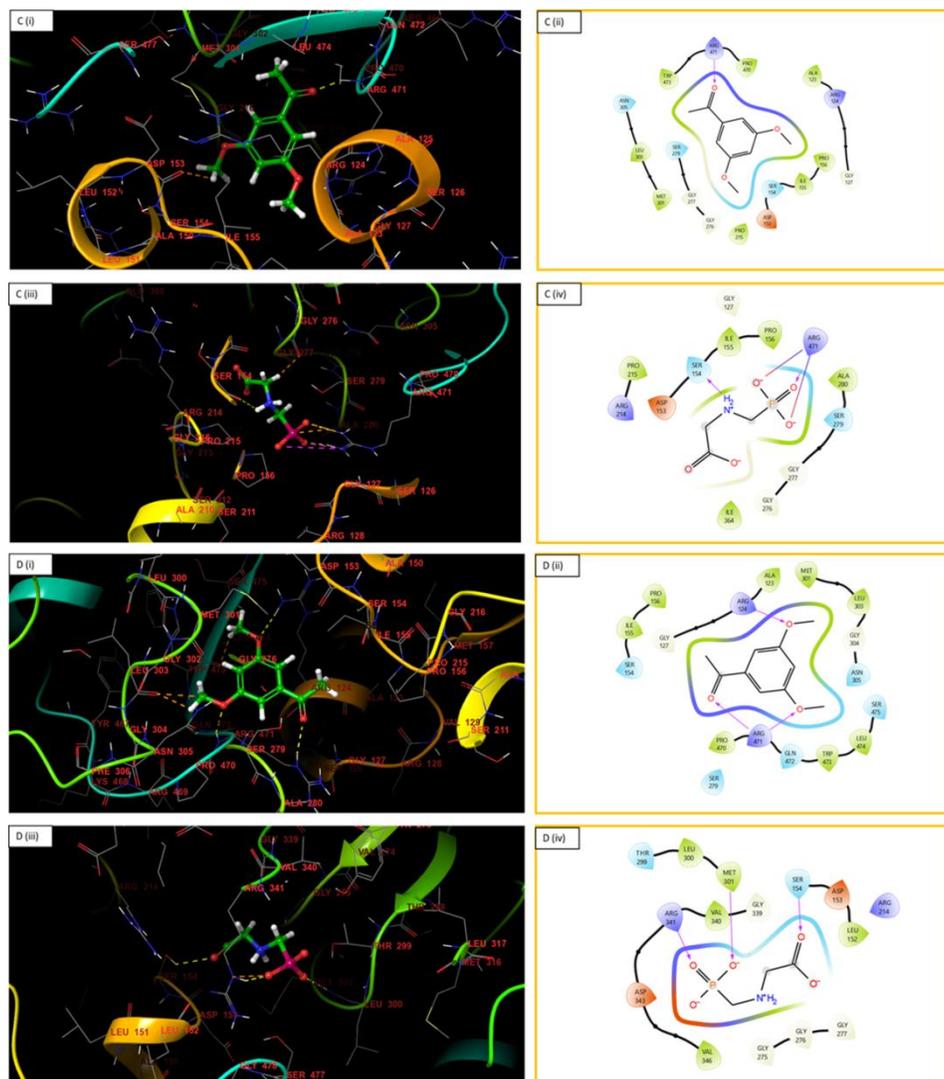
Fig. 3. Interactions between the target receptors and selected compounds representing in 2D (left) and 3D (right) format. Representing the compounds C. GLS (i, ii) CID: 95997, C. GLS (iii, vi) CID: 3496 (control), and D. PSIID1 (i, ii) CID: 95997, D. PSIID1 (iii, iv) CID: 3496 (control) inside the protein.

simulations involved with the apoproteins, the next 4 simulations were with the top lead compounds (from molecular docking) bound to their respective target proteins, forming protein–ligand complexes. The remaining 4 simulations were conducted with glyphosate (CID: 3496) as a control, allowing a comparative analysis between glyphosate-bound complexes and lead compound-bound complexes. The results of the MD simulations were analyzed by examining the radius of gyration (Rg), solvent-accessible surface area (SASA), root-mean-square deviation (RMSD), and root-mean-square fluctuation (RMSF).

Table 4. Molecular docking scores and the amino acid residues involved in binding between the target proteins and the selected compounds.

Protein name	CID	Phytochemical Name	Docking score (kcal mol⁻¹)	H-bond	Polar bond	Hydrophobic bond	Other bonds
Acetohydroxy acid synthase	543891	CIS-2,4-DIMETHYLTHIANE, S,S-DIOXIDE	-5.546	-	THR854, GLN591, ASN606	PHE609, PHE610, VAL624, VAL626, TRP820, ILE779	ASP778
	3496	Glyphosate	-2.225	-	THR776, THR854	TRP820, ILE779, VAL624, TYR625, VAL626, PHE609	ASP778, ARG819
Cellulose Synthase	22211625	CHOLEST-5-EN-3-OL, (3.ALPHA.)-, TMS DERIVATIVE	-7.539	-	HIE933, ASN921, THR854, THR776, THR628, GLN591, GLN816, ASN606	TRP925, PHE924, TYR857, ILE779, VAL624, TYR625, VAL626, TRP820, VAL817, PHE609, PHE610	ASP778, GLY627, LYS533, ASP557, ARG819, ARG813, GLY928
	3496	Glyphosate	-3.878	TRP820, ASP778	THR776	VAL626, ILE779	LYS533, GLY627
Glutamine Synthase	95997	3',5'-DIMETHOXYACETOPHENONE (CID-95997)	-7.082	ARG471	ASN305, SER279, SER154	LEU303, MET301, TRP473, PRO470, ALA123, PRO156, ILE155, PRO215	ARG124, GLY127, ASP153, GLY276, GLY277
	3496	Glyphosate	-3.88	SER154, ARG471	SER279	PRO215, ILE155, PRO156, ALA280, ILE364	ARG214, ASP153, GLY127, GLY277, GLY276
Photosystem II D1	95997	3',5'-DIMETHOXYACETOPHENONE (CID-95997)	-7.238	ARG124, ARG471	SER154, ASN305, SER475, GLN472, SER279	PRO156, ILE155, ALA123, MET301, LEU303, LEU474, TRP473, PRO470	GLY127, GLY304
	3496	Glyphosate	-4.074	ARG341, MET301, SER154	THR299	LEU300, MET301, VAL340, LEU152, VAL346	GLY339, ASP153, ARG214, GLY277, GLY276, GLY275, ASP343

Table 5. QSAR model results for predicting the bioactivity of the chosen lead compounds.

SI	CID	Phytochemical Name	Pa	Pi	Activity
1.	95997	3',5'-DIMETHOXYACETOPHENONE	0,136	0,044	1-Aminocyclopropane-1-carboxylate deaminase inhibitor (Gamalero et al. 2023)
			0,132	0,031	Acetolactate synthase inhibitor (Dezfulian et al. 2017)
			0,203	0,035	Cellulase inhibitor (Fan et al. 1966)
			0,290	0,041	Glutaminase inhibitor (Siehl et al. 1997)
2.	543891	CIS-2,4-DIMETHYLTHIANE, S,S-DIOXIDE	0,165	0,085	Microtubule formation inhibitor (Ishida et al. 2021)
3.	22211625	CHOLEST-5-EN-3-OL, (3.ALPHA.)-, TMS DERIVATIVE	0,077	0,006	Na⁺ K⁺ transporting ATPase inhibitor (Apse et al. 2007)

Furthermore, the protein-ligand interactions were tracked and visualized throughout the simulation. RMSD quantifies the average atomic displacement over time compared to a reference structure (Benson et al. 2012). For protein-ligand complexes, RMSD values

between 1-3 Å are generally considered acceptable. If the RMSD value exceeds 3Å, it suggests a conformational shift in the protein structure. To evaluate the structural changes in the target proteins, a total of 12 molecular dynamics simulations were performed over a 50-nanosecond time frame. These simulations assessed the conformational stability of proteins complexed with both the selected lead compounds and the control compound (CID: 3496) shown in the Table 6.

Table 6. Highest, lowest, and average RMSD values for the target protein-ligand complexes.

Protein Name	Compound CID	Lowest RMSD value (Å)	Highest RMSD value (Å)	Average RMSD (Å)
Acetohydroxyacid synthase	Apo	4.502	6.368	4.988
	543891	3.705	4.848	4.323
	3496	4.038	5.575	4.820
Cellulose Synthase	Apo	11.5	15.263	12.995
	22211625	10.793	15.849	13.672
	3496	13.023	15.569	13.690
Glutamine Synthase	Apo	9.279	16.447	10.402
	95997	9.678	18.446	12.294
	3496	6.884	17.543	11.080
Photosystem II D1	Apo	5.371	16.06	9.94
	95997	12.545	16.509	13.124
	3496	13.684	16.195	13.203

Root Mean Square Fluctuation (RMSF) is an important measure of localized structural changes in a protein when it interacts with other molecules (Fuglebakk et al. 2012). It helps determine changes in protein flexibility when certain compounds bind to specific residual sites. RMSF values were calculated and visualized in Fig. 4 to assess structural fluctuations in the apoproteins and target receptors when bound to CID: 95997, CID: 543891, CID: 22211625, and CID: 3496. The selected compounds in Figure 5 exhibited peak fluctuations at residue positions shown in table 7, indicating regions of the protein that underwent the most significant changes during the simulation. Overall, the RMSF analysis showed only slight variations between protein-ligand complexes.

The radius of gyration (Rg) describes how the atoms in a protein-ligand complex are distributed along its central axis (Flores et al. 2011). It is a crucial parameter for assessing the structural behavior of a macromolecule, as it indicates changes in compactness within the complex. To evaluate structural stability, the Rg values for CID: 95997, CID: 543891, CID: 22211625   in complex with the target protein were analyzed over a 50-nanosecond simulation, as illustrated in (Fig. 5A-D). The average Rg are shown in table 8, suggesting that the binding of the selected compounds does not induce significant conformational changes at the protein's active site.
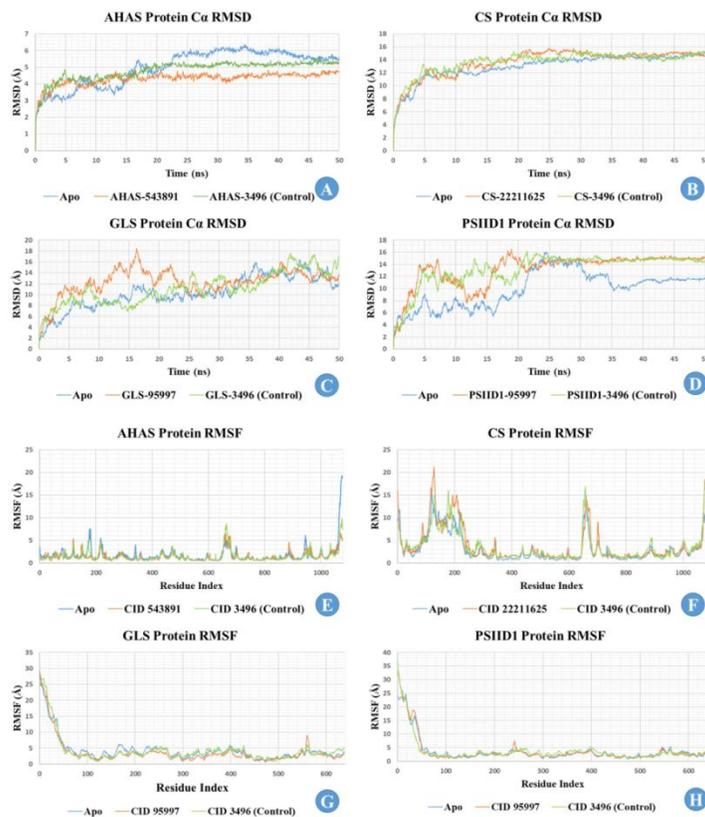
Fig. 4. RMSD (A-D) and RMSF (E-H) values of target proteins in complex with ligand and control. (A) AHAS -
543891(Blue), AHAS - 3496(Orange); (B) CS - 22211625 (Blue), CS - 3496 (Orange); (C) GLS - 95997 (Blue),
GLS - 3496 (Orange); (D) PSIID1 - 95997 (Blue), PSIID1 - 3496 (Orange) ;(E) AHAS - 543891 (Blue), AHAS -
3496 (Orange); (F) CS - 22211625 (Blue), CS - 3496 (Orange); (G) GLS - 95997 (Blue), GLS - 3496 (Orange);
(H) PSIID1 - 95997 (Blue), PSIID1 - 3496 (Orange).

Table 7. RMSF values for the target proteins when bound to the selected ligands.

| Target Protein	Compound CID	Peak area residues	Lowest RMSF value position	Average RMSD (Å)
Acetohydroxyacid synthase	Apo	SER181, CYS658, GLY947, ILE1076	550, 633	1.670
	543891	GLY121, GLY149, VAL218, ARG662, SER678, ILE888, ASP962, ASP1070	576	1.405
	3496	TYR174, THR217, SER666, ILE1076	585	1.466
Cellulose Synthase	Apo	GLY8, PRO120, SER661, VAL1071	629	3.086
	22211625	MET1, ASN128, GLY194, ASP208, SER661, GLY702, ASN1077	624	3.721
	3496	TYR129, HIS179, GLY224, CYS658, ASN1077	354, 591	3.498
Glutamine Synthase	Apo	MET1, SER6, SER31, ARG167, LYS402	120, 473	4.368
	95997	MET1, GLU561	474	3.680
	3496	VAL9, GLN259, LYS399, GLY428, GLU561	124, 491	4.311
Photosystem II D1	Apo	MET1, THR18, THR36, ARG546, SER564, TYR639	299, 475	3.733
	95997	MET1, ARG33, PRO242, TYR639	117, 487	3.722
	3496	MET1, GLY403, TYR639	117, 487	3.804
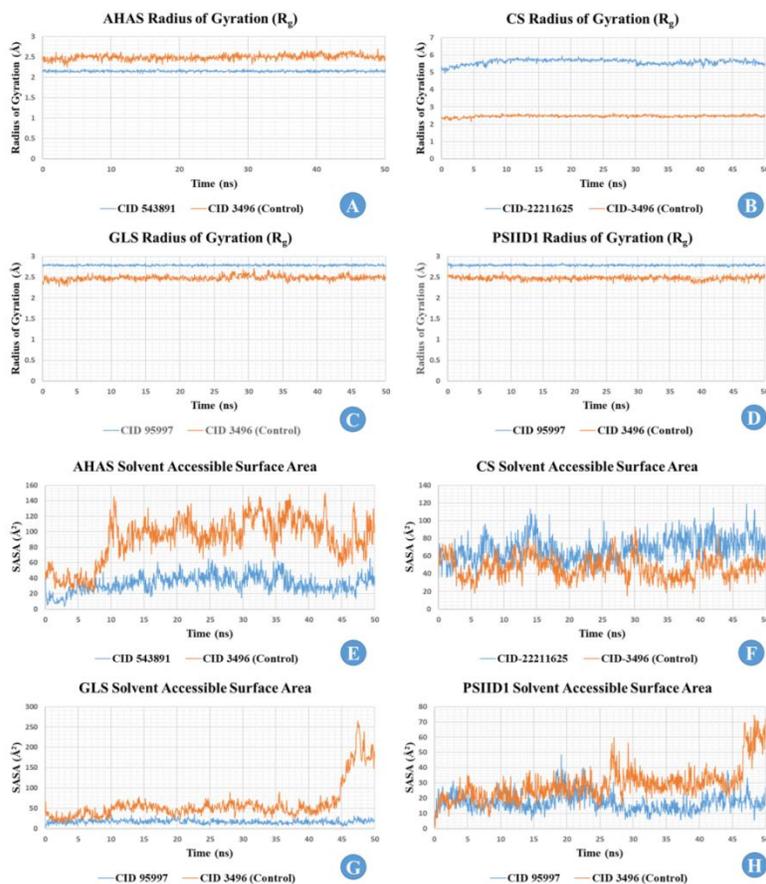
Fig. 5. Rg (A - D) and SASA (E-H) of the protein-ligand complexes. (A) AHAS - 543891 (Blue), AHAS - 3496 (Orange); (B) CS - 22211625 (Blue), CS - 3496 (Orange); (C) GLS - 95997 (Blue), GLS - 3496 (Orange); (D) PSIID1 - 95997 (Blue), PSIID1 - 3496 (Orange) ;(E) AHAS - 543891 (Blue), AHAS - 3496 (Orange); (F) CS - 22211625 (Blue), CS - 3496 (Orange); (G) GLS - 95997 (Blue), GLS - 3496 (Orange); (H) PSIID1 - 95997 (Blue), PSIID1 - 3496 (Orange).

Table 8. Average radius of gyration values for the target proteins when bound to the selected ligands.

Target Protein	Compound CID	Average Radius of Gyration value (Å)
Acetohydroxyacid synthase	543891	2.150
	3496	2.496
Cellulose Synthase	22211625	5.601
	3496	2.466
Glutamine Synthase	95997	2.788
	3496	2.483
Photosystem II D1	95997	2.787
	3496	2.479

Solvent-accessible surface area (SASA) is important for understanding the structure and function of large biological molecules (Ali et al. 2014). Surface amino acids often form active sites or interact with other molecules and ligands. SASA helps us understand protein-ligand complexes and whether molecules are hydrophilic or hydrophobic. SASA values were calculated and are shown in (Fig. 5E-H) to analyze the interactions in the protein-ligand complexes formed with CID: 95997, CID: 543891, and CID: 22211625. The findings revealed that certain amino acid residues exhibited a high level of exposure to the selected molecules in the complex system. The average SASA value ranged between Acetohydroxyacid synthase average between (32.972-90.439) $Å^2$, Cellulose Synthase average between (46.835-68.167) $Å^2$, Glutamine Synthase average between (16.773-60.278) $Å^2$, Photosystem II D1 average between (16.984-28.811) $Å^2$, indicating the extent of solvent interaction with the protein surface.

Pre-emergence tests showed that the *Manilkara zapota* crude extract significantly hindered *Parthenium hysterophorus* seed germination, with the level of inhibition depending on the extract concentration (Fig. 6A-B). At a concentration of 0.05 g/ml, the extract achieved reduction in seed germination after 5 days. Furthermore, Molecular Docking analysis identified key bioactive compounds contributing to this phytotoxic effect. Notably, 3',5'-DIMETHOXYACETOPHENONE (CID: 95997), CIS-2,4-DIMETHYL THIANE, S,S-DIOXIDE (CID: 543891) and CHOLEST-5-EN-3-OL, (3.ALPHA.)-, TMS DERIVATIVE (CID: 22211625) significantly suppressed the seed germination of *P. hysterophorus* (Table 9).
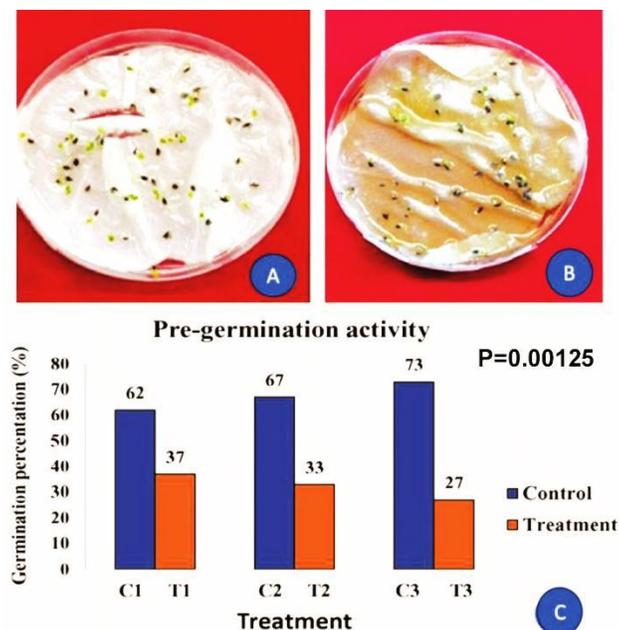

Fig. 6. Pre-germination activity and significant test of control (A) and treatment (B) of *M. zapota* leaf extract on *P. hysterophorus* seeds. (A) Control, (B) Treatment, (C) Germination Inhibition graph.

Table 9. Pre-germination activity data table.

Treatment group		No. of seed sown	No. of seed germination	Germination percentage (%)
Control (water only)	C1	45	28	62%
	C2	45	30	67%
	C3	45	33	73%
Treatment (extract)	T1	45	17	37%
	T2	45	15	33%
	T3	45	12	27%

The graph in the figure 6 allows for a direct visual comparison of the germination percentages of *Parthenium hysterophorus* seeds between the control and treatment groups across the three time points. The blue bars show the germination percentage of the control group at each time point (Fig. 6C). This helps establish a baseline for normal germination. The orange bars reveal how the treatment affected germination compared to the control at each time point. The differences in height between the blue and orange bars at each time point indicate the treatment's effect on germination. Larger differences suggest a stronger treatment effect. While the graph provides a clear visual representation, further statistical analysis (e.g., t-tests) would be necessary to determine if the observed differences in germination percentages are statistically significant. The t-test score for seed germination percentage is 8.12. The t-distribution table was used to find the p-value. The p value in this case is 0.00125 which is required to determine the statistically significant result. Here the p value is significant as it is <0.05. So, the difference between control and treatment group are statistically significant and therefore the crude extract has inhibitory effect on *P. hysterophorus* seed germination. CIS-2,4-DIMETHYLTHIANE, S,S-DIOXIDE (CID-543891), CHOLEST-5-EN-3-OL, (3.ALPHA.)-, TMS DERIVATIVE (CID-22211625) and 3',5'-DIMETHOXYACETOPHENONE (CID-95997) can be responsible for this effect as these compounds have potential binding score with target proteins.

Bioherbicides are emerging as a sustainable alternative to synthetic chemical herbicides. These natural herbicides, derived from microorganisms like bacteria, fungi, or viruses, or from plant-based products, offer a promising solution amid growing concerns over environmental health, biodiversity, human safety, and the long-term sustainability of agriculture (Hasan et al. 2021). The overuse of synthetic herbicides has caused significant environmental pollution, contaminating air, water, and soil. Pesticide runoff harms aquatic ecosystems, disrupting the food chain (Gupta et al. 2025). Conventional herbicides like glyphosate and atrazine can persist in the environment, bioaccumulating in wildlife and even humans (Mahler et al. 2017). In contrast, bioherbicides, sourced from naturally occurring microorganisms or organic compounds, typically break down into non-toxic or much less harmful products, offering a lower ecological footprint. They are biodegradable, minimizing the risk of long-term environmental contamination (Bailey 2014, Hasan et al. 2021).

Chemical herbicides, while targeting unwanted weeds, can also harm non-target plants, leading to a reduction in biodiversity within agricultural systems. The indiscriminate application of these herbicides can result in the loss of beneficial plant species that provide critical habitats for insects, birds, and other wildlife (Breeze et al. 1999). The over-reliance on synthetic herbicides has led to the development of herbicide-resistant weed species, which reduces herbicide effectiveness. This increases herbicide use and escalates environmental harm (Cerdeira et al. Heap 2014). Bioherbicides can mitigate herbicide resistance, as they often act through different mechanisms, making them suitable for integrated weed management (IWM) strategies. By reducing selection pressure on weeds, bioherbicides helps slow down the development of resistance (Camargo et al. 2019).

Although the initial costs for research and development of bioherbicides can be high, their long-term use is often more economically sustainable compared to chemical herbicides. The costs associated with environmental cleanup, healthcare from chemical herbicide poisoning, and biodiversity loss from synthetic herbicides can be substantial (Poudel et al. 2020). Bioherbicides offer a cleaner, more cost-effective alternative, minimizing the need for extensive remediation efforts (Lynch et al. 2006). Increasing consumer demand for organic and pesticide-free products, driven by health and environmental concerns, has further incentivized the adoption of bioherbicides. Bioherbicides are essential in organic farming, where the use of synthetic pesticides, including herbicides, is prohibited. As such, bioherbicides help meet the growing demand for organic produce, offering a non-chemical alternative to weed control. Farmers using bioherbicides can market their products as environmentally friendly, potentially increasing the market value of their crops. The use of synthetic herbicides has been linked to numerous health issues, from acute poisoning to chronic conditions like cancer, endocrine disruption, and neurological disorders (Mostafalou et al 2017). Agricultural workers, in particular, face higher risks due to regular exposure to these chemicals. While some bioherbicides can still pose health risks (Eddaya et al. 2015), such as allergic reactions or respiratory issues when mishandled, their overall toxicity to humans is much lower compared to synthetic herbicides. Bioherbicides offer more flexible and adaptive solutions to weed control, better suited to the changing environmental conditions (Hasan et al. 2021). Using them promotes climate-resilient agriculture, which is crucial for maintaining food security as the climate continues to changes (Yiridoe et al. 2005).

However, by examining the binding energy and stability using dynamic modeling with common weeds target proteins including Acetohydroxyacid Synthase, Cellulose Synthase, Glutamine Synthase, and Photosystem II D1, we have demonstrated for the first time in our study that *Manilkara zapota* leaf extract phytochemicals may be a potential inhibitor of the weeds target. Our findings thus demonstrated that these substances can also be utilized as a possible potential applicant for herbicide. In this study, all complexes including reference had relatively similar and consistent values

throughout 50 ns, and also perfectively superimposed each other. Higher Pa values of selected lead phytochemicals of QSAR model suggest stronger pharmacological activity and greater potential for experimental development. The less variation in the value of the radius of gyration of target weed proteins with the control glyphosate (CID-3496) suggested that proteins are compactly packed and binding of inhibitors do not affect the rigidity of the protein. The analysis of SASA and hydrogen bonding also supports the stable binding of the small molecules to the protein. The results of these simulations clearly show that the prominent phytochemicals in *M. zapota* have strong inhibitory potential across numerous herbicidal pathways. Detailed computational investigations offered significant structural insights into the active-site residues implicated in inhibition and highlighted the superior interaction patterns of substances such as CIS-2,4-DIMETHYLTHIANE, S,S-DIOXIDE (CID-543891), CHOLEST-5-EN-3-OL, (3.ALPHA.)-, TMS DERIVATIVE (CID-22211625) and 3',5'-DIMETHOXYACETOPHENONE (CID-95997). Crude extracts from *M. zapota* were prepared and their herbicidal activity evaluated against weed species such as *Parthenium hysterophorus* through seed germination. The study highlights *M. zapota* as a promising source of bioherbicidal compounds, offering an environmentally sustainable alternative to synthetic herbicides. Thus, this theoretical study implies that these bioactive ingredients could be attractive natural herbicide candidates.

The study highlights *M. zapota* as a promising source of bioherbicidal compounds, offering an environmentally sustainable alternative to synthetic herbicides. Our germination inhibition study shows that *M. zapota* as a promising plant with pre-emergence herbicidal activity. This opens new perspectives on the application of *M. zapota* plant extracts as botanical herbicides for weed management. Thus, this theoretical study implies that these bioactive ingredients could be attractive natural herbicide candidates, providing a solid foundation for future innovation and development of eco-friendly, plant-based weed-management solutions.

Acknowledgment

References

Araniti, F, Mancuso R, **Lupini A**, **Giofrè SV**, **Sunseri F**, **Gabriele B** and **Abenavoli MR** (2015) Phytotoxic Potential and Biological Activity of Three Synthetic Coumarin Derivatives as New Natural-Like Herbicides. Molecules **20**(10): 17883-17902.

Ali SA, Hassan MI, Islam A and **Ahmad F** (2014) A review of methods available to estimate solvent-accessible surface areas of soluble proteins in the folded and unfolded states. **15**(5): 456-476.

Bailey KL (2014) The bioherbicide approach to weed control using plant pathogens. Integrated pest management, Elsevier: 245-266.

Bailey LH and **Bailey EZ** (1976) Hortus Third; a concise dictionary of plants cultivated in the United States and Canada.

Benson NC and **Daggett V** (2012) A comparison of multiscale methods for the analysis of molecular dynamics simulations. J. Phys. Chem. B. **116**(29): 8722-8731.

Breeze VG, Marshall EJP, Hart A, Vickery JA, Crocker J, Walters K, Packer J, Kendall D, Fowbert J and **Hodkinson D** (1999) Assessing pesticide risks to non-target terrestrial plants." A desk study. Commission PN0923. MAFF Pesticides Safety Directorate.

Battaglino B, Grinzato A and **Pagliano C** (2021) Binding properties of photosynthetic herbicides with the QB site of the D1 protein in plant photosystem II: a combined functional and molecular docking study. Plants **10**(8): 1501.

Buffon G, Lamb TI, Lopes MCB, Sperotto RA and **Timmers LFSM** (2020). Push it to the limit: identification of novel amino acid changes on the acetolactate synthase enzyme of rice that putatively confer high level of tolerance to different Imidazolinones. Front. Bioeng. Biotech. **8**: 73.

Camargo AF, Stefanski FS, Scapini T, Weirich SN, Ulkovski C, Carezia C, Bordin ER, Rossetto V, Júnior FR and **Galon L** (2019) Resistant weeds were controlled by the combined use of herbicides and bioherbicides. Environ. Qual. Manag. **29**(1): 37-42.

Carvalho MSS, Andrade-Vieira LF, Santos FEd, Correa FF, Cardoso MdG and **Vilela LR** (2019) Allelopathic potential and phytochemical screening of ethanolic extracts from five species of *Amaranthus spp*. in the plant model *Lactuca sativa*. Sci. Hort. **245**: 90-98.

Cerdeira AL and **Duke SO** (2006) The current status and environmental impacts of glyphosate-resistant crops: a review. J. Environ. Qual. **35**(5): 1633-1658.

Chengxu, W, Mingxing Z, Xuhui C and **Bo Q** (2011) Review on Allelopathy of Exotic Invasive Plants. Procedia Eng. **18**: 240-246.

Cordeau S, Triolet M, Wayman S, Steinberg C and **Guillemin JP** (2016) Bioherbicides: Dead in the water? A review of the existing products for integrated weed management. Crop Prot. **87**: 44-49.

Donn G and **Köcher H** (2002) Inhibitors of glutamine synthetase. In Herbicide classes in development: mode of action, targets, genetic engineering, chemistry (pp. 87-101). Berlin, Heidelberg: Springer Berlin Heidelberg.

Eddaya T, Boughdad A, Becker L, Chaimbault P and **Zaïd A** (2015) Utilisation et risques des pesticides en protection sanitaire de la menthe verte dans le Centre-Sud du Maroc (Use and risks of pesticides in sanitary protection of spearmint in south-central Morocco)." J. Mater. Environ. Sci. **6**(3): 656-665.

Fayek NM, Monem ARA, Mossa MY, Meselhy MR and **Shazly AH** (2012) Chemical and biological study of *Manilkara zapota* (L.) Van Royen leaves (Sapotaceae) cultivated in Egypt. J. Pharm. Pharmacogn. Res. **4**(2): 85.

Feng G, Chen M, Ye HC, Zhang ZK, Li H, Chen LL, Chen XL, Yan C and **Zhang J** (2019) Herbicidal activities of compounds isolated from the medicinal plant *Piper sarmentosum*. Ind. Crops Prod. **132**: 41-47.

Flamini G (2012) Natural Herbicides as a Safer and More Environmentally Friendly Approach to Weed Control: A Review of the Literature Since 2000. Studies in Natural Products Chemistry. R. Atta ur, Elsevier. **38**: 353-396.

Flores SC and **Gerstein MB** (2011) Predicting protein ligand binding motions with the conformation explorer. BMC Bioinfor. **12**: 1-12.

Fuglebakk E, Echave J and **Reuter N** (2012) Measuring and comparing structural fluctuation patterns in large protein datasets. Bioinformatics **28**(19): 2431-2440.

Gam S, Ahmed R, Kashyap B, Sarma H, Sahariah BJ, Bora NS, Deka K, Gogoi B and **Dutta KN** (2024) A systematic review on traditional use, phytochemistry and pharmacological activities of *Manilkara zapota*. Pharmacological Research - Natural Products **4**: 100062.

Gupta RC and **Gupta PK** (2025) Toxicity of herbicides. Veterinary toxicology, Elsevier: 565-579 Academic Press.

Hasan M, Ahmad-Hamdani MS, Rosli AM and **Hamdan H** (2021) Bioherbicides: An Eco-Friendly Tool for Sustainable Weed Management. Plants. **10**(6): 1212.

Heap I (2014) Global perspective of herbicide-resistant weeds. Pest Manag. Sci. **70**(9): 1306-1315.

Heatley NG (1944) A method for the assay of penicillin. Biochem. J. **38**(1): 61.

Kaab SB, Lins L, Hanafi M, Rebey IB, Deleu M, Fauconnier ML, Ksouri R, Jijakli MH and **Clerck CD** (2020) *Cynara cardunculus* Crude Extract as a Powerful Natural Herbicide and Insight into the Mode of Action of Its Bioactive Molecules. Biomolecules **10**(2): 209.

Lim CJ, Basri M, Ee GC and **Omar D** (2017) Phytoinhibitory activities and extraction optimization of potent invasive plants as eco-friendly weed suppressant against *Echinochloa colona* (L.) Link. Ind. Crops Prod. **100**: 19-34.

Lynch SM, Rusiecki JA, Blair A, Dosemeci M, Lubin J, Sandler D, Hoppin JA, Lynch CF and **Alavanja MC** (2006) Cancer Incidence among Pesticide Applicators Exposed to Cyanazine in the Agricultural Health Study. Environ. Health Perspect. **114**: 1248-1252.

Mahler BJ, Van Metre PC, Burley TE, Loftin KA, Meyer MT and **Nowell LH** (2017) Similarities and differences in occurrence and temporal fluctuations in glyphosate and atrazine in small Midwestern streams (USA) during the 2013 growing season. Sci. Total Environ. **579**: 149-158.

Mandels M and **Reese E** (2003) Inhibition of Cellulases. Annu. Rev. Phytopathol. **3**: 85-102.

Mostafalou S and **Abdollahi M** (2017) Pesticides: an update of human exposure and toxicity. Arch. Toxicol. **91**(2): 549-99.

McCurdy JD, McElroy JS and **Flessner ML** (2013) Differential response of four *Trifolium* species to common broadleaf herbicides: implications for mixed grass-legume swards. Weed Technol. **27**(1): 123-128.

Nguyen TLT, Ly HG, Le ATK and **Tran BG** (2025) Antioxidant, antibacterial, anti-inflammatory, and anticancer activities of the methanol extract from *Manilkara zapota* leaves collected in Vietnam. Ho Chi Minh City Open Univ. J. Sci. - Eng. Technol. **16**(1).

Nandula VK, Giacomini DA and **Ray JD** (2020) Resistance to acetolactate synthase inhibitors is due to a W 574 to L amino acid substitution in the ALS gene of redroot pigweed and tall waterhemp. Plos one **15**(6): p.e0235394

Poudel S, Poudel B, Acharya B and **Poudel P** (2020) Pesticide use and its impacts on human health and environment. Environ. Ecosyst. Sci. **4**(1): 47-51.

Ribeiro RC, Feitoza RBB, Lima HRP and **Geraldo de Carvalho M** (2015) Phytotoxic effects of phenolic compounds on *Calopogonium mucunoides* (Fabaceae) roots. Aust. J. Bot. **63**(8): 679-686.

Shukla R and **Tripathi T** (2021) Molecular dynamics simulation in drug discovery: opportunities and challenges. pp. 295-316.

Soltys D, Gniazdowska A, Bogatek R and **Krasuska U** (2013) Allelochemicals as Bioherbicides Present and Perspectives. Herbicides - Current Research and Case Studies in Use. A. Price and J. Kelton. London, Intech Open.

Shahraki SH, Javar FM and **Rahimi M** (2023) Quantitative and Qualitative Phytochemical Analysis of *Manilkara zapota* (Sapodilla) Extract and Its Antibacterial Activity on Some Gram-Positive and Gram-Negative Bacteria. Scientifica **1**: 5967638.

Shui G, Wong SP and **Leong LP** (2004) Characterization of antioxidants and change of antioxidant levels during storage of *Manilkara zapota* L. J. Agric. Food Chem. **52**(26): 7834-7841.

Sabba RP and **Vaughn KC** (1999) Herbicides that inhibit cellulose biosynthesis. Weed Sci. **47**(6): 757-763.

Stidham MA (1991) Herbicides that inhibit acetohydroxyacid synthase. Weed Sci. **39**(3): 428-434

Shah S, Lonhienne T, Murray CE, Chen Y, Dougan KE, Low YS, Williams CM, Schenk G, Walter GH, Guddat LW and **Chan CX** (2022) Genome-guided analysis of seven weed species reveals conserved sequence and structural features of key gene targets for herbicide development. Front. Plant Sci. **13**: 909073.

Tulloch A, Goldson-Barnaby A, Bailey D and **Gupte S** (2020) *Manilkara zapota* (Naseberry): medicinal properties and food applications. Int. J. Fruit Sci. **20**(sup2): S1-S7.

Teixeira MM, Aguiar GR, da Silva JM, da Silva KTM, Siebeneichler SC, Júnior OJF, Lima CSL, da Silveira Bastos IMA, de Sousa AS and **de Oliveira M** (2024) Photosystem II inhibitor herbicides. Observatório De La Economía Latinoamericana **22**(7): e5856-e5856.

Yiridoe EK, Bonti-Ankomah S and **Martin RC** (2005) Comparison of Consumer Perceptions and Preference Toward Organic Versus Conventionally Produced Foods: A Review and Update of the Literature. Renew. Agric. Food Syst. **20**: 193-205.